



A Measurement of Top Quark Mass Using MET + Jets Events With Full CDF Data Set 8.7 fb^{-1}

The CDF Collaboration
URL <http://www-cdf.fnal.gov>
(Dated: May 16, 2012)

We present a measurement of top-quark mass using CDF full data of 8.7 fb^{-1} of Tevatron's $p\bar{p}$ collisions collected by the CDF detector at Fermilab. We use a neural network to select the events, which have a signature of $\cancel{E}_T + \text{jets}$ in the final state after all cuts. Data events are triggered by high jet-multiplicities, and the background is modeled from data. The measurement is based on a three-dimensional template method, and reconstructs three observables, which are m_t^{reco} , the reconstructed top mass, $M_t^{\text{reco}(2)}$ a second reconstructed top mass, and m_{jj} , which is the invariant mass of two jets from the hadronic W decays and provides an *in situ* improvement in the determination of jet energy scale. We perform a minimum Log-likelihood fit to the data and measure the top-quark mass to be $173.9 \pm 1.9 \text{ GeV}/c^2$.

Preliminary Results of TMT using 8.7 fb^{-1}

I. INTRODUCTION

This note describes a measurement of the mass of the top quark using $p\bar{p}$ collisions at $\sqrt{s} = 1.96$ TeV with the CDF detector at the Tevatron. The mass of the top quark is of much interest to particle physicists, both because the top quark is the heaviest known fundamental particle, and also because a precise measurement of the top quark mass helps constrain the mass of the Higgs boson. Top quarks are produced predominantly in pairs at the Tevatron, and in the Standard Model decay nearly 100% of the time to a W boson and a b quark. The topology of a $t\bar{t}$ event is determined by the decay of the two W bosons, as each W boson can decay to a lepton-neutrino pair ($l\nu$) or to a pair of quarks (qq'). We look for events triggered by a large missing E_T and multiple jets, typically those with one W boson decaying hadronically and the other decaying leptonically. The CDF detector is described in [1]. This analysis is based on a similar measurement of the top quark mass using 5.6 fb^{-1} of CDF data [2], but has improvement in selecting and reconstructing the candidate events.

Our measurement is a template-based measurement, meaning that we compare quantities in data with distributions from simulated MC events to find the most likely top quark mass. We reconstruct the top quark mass for each event by fitting a χ^2 function fitter, and choose the masses with the best and second-best χ^2 values as the two kinematic variables for top quark mass. We also reconstruct a (m_{jj}) from the decay products of W resonance since it is sensitive to possible miscalibration of (jet energy scale) JES in the CDF detector.

Monte Carlo samples generated with 76 different M_{top} are run through a full CDF detector simulation assuming 29 possible shifts in Δ_{JES} . The values of the three sets of observables in data are compared to each point in the MC grid using a non-parametric approach based on Kernel Density Estimation (KDE). Local Polynomial Smoothing is used to smooth out these points and calculate the probability densities at any arbitrary value of M_{top} and Δ_{JES} . An unbinned likelihood fit is used to measure M_{top} and profile out Δ_{JES} .

II. EVENT SELECTION

At the trigger level, the candidate events are selected by requiring high jet-multiplicities. Offline, a series of clean up cuts are applied first. The events are required to have a missing E_T significance $> 3 \text{ GeV}^{1/2}$ and events with tight or loose leptons are rejected, so that the measurement is independent of other CDF top quark mass measurements. We also require at least four jets and at most six jets in the final state. A neural network training with two hidden layers is performed after the clean up selection to enhance the signal-to-background ratio.

To improve the statistical power of the method, we divide each event sample into two subsamples, depending on the number of jets identified as arising from the hadronization and decay of b quarks. The SECVTX [7] algorithm uses the transverse decay length of tracks inside jets to tag jets as coming from b quarks.

III. BACKGROUND ESTIMATION

We use a data driven background estimation in this analysis. Because the probability for a jet to be identified as a b-quark jet is different for the jets in the $t\bar{t}$ events and in the QCD production with heavy flavor process, which dominates the background process of this analysis, we can use this feature to estimate the background rate in the data. We build a per-jet b-tag rate matrix from a $t\bar{t}$ -signal-negligible data sample, which consists of events with exactly three jets, and parameterize the b-tag probability as a function of three jet characteristics: jet transverse energy, jet number of tracks, and the MET projection along the jet direction.

We apply the btag rate matrix to events at higher jet-multiplicities to estimate the background rate. At higher jet multiplicities, however, the $t\bar{t}$ signal contamination is not negligible. We use an iterative correction method to remove the sizable $t\bar{t}$ events in each jet bin in order to correct our background prediction. We validate our background estimation by comparing the expected and observed number of b-tagged events at different jet-multiplicities at the background dominant region with Neural Network output less than 0.4, as shown in Table I.

TABLE I: Expected and observed number of b-tagged events at different jet-multiplicities at the background dominant region NNoutput < 0.4 .

Jet Multiplicity	3 jets	4 jets	5 jets	6 jets	≥ 7 jets
Observed	13360	34967	20863	8729	5369
Expected	12930.4	34444.4	20597.9	8653.36	5217.32
Difference(%)	3.2	1.5	1.3	0.8	2.8

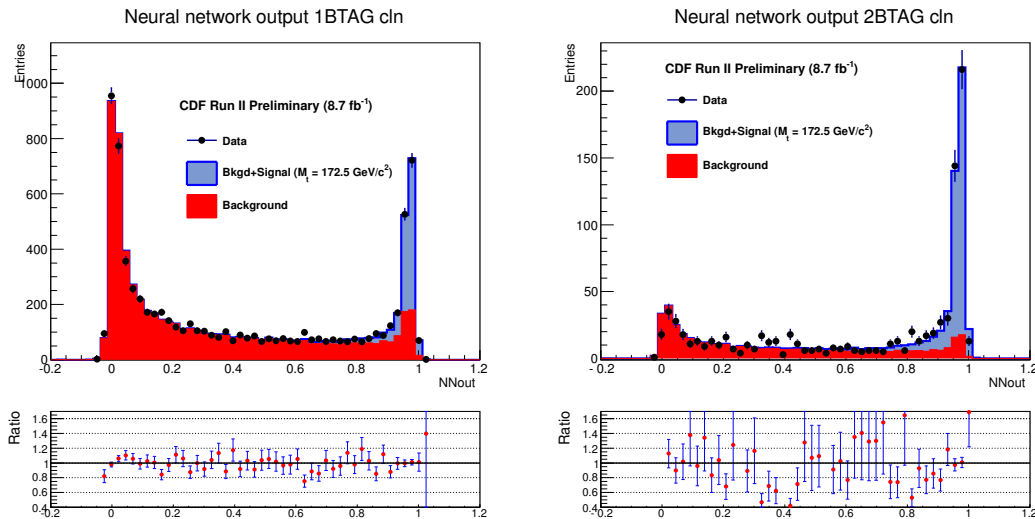


TABLE II: Expected and Observed number of events after all cuts within $4 \leq n_{\text{jets}} \leq 6$.
CDF II Preliminary 8.7 fb^{-1}

b-tagging	jet-multiplicity	Signal	Background	Total Expected	Observed
1tag	4 jets	427.1 ± 50.3	262.9 ± 23.0	690.0 ± 55.3	761
	5 or 6 jets	801.0 ± 70.8	450.4 ± 29.2	1251.4 ± 76.6	1341
2tag	4 jets	179.0 ± 23.8	43.5 ± 11.4	222.51 ± 26.3	225
	5 or 6 jets	373.5 ± 37.4	125.1 ± 23.4	498.6 ± 44.1	550

We calculate the number of background events for 1tag and 2tag event samples respectively. The calculation involves a btagging correction factor that takes into account the fact that in QCD events heavy flavor quark tend to come in pairs, which enhances the 2tag probability of an event. After the two correction procedures mentioned above, we can estimate the background rates for both 1tag and 2tag event samples. We plot the Neural Network output on Fig. III, based on which we require the $\text{NNout} > 0.9$ for 1tag events, and $\text{NNout} > 0.8$ for 2tag events to reject a considerable amount of background events. We calculate the estimated number of background events on Table II, which also shows the total number of expected and observed events. Events here are required to pass all the cuts in the signal region, which includes the requirement of $4 \leq n_{\text{jets}} \leq 6$.

IV. JET ENERGY SCALE

We describe in this section the *a priori* determination of the jet energy scale uncertainty by CDF that is used later in this analysis. More information on JES, calibration and uncertainty can be found in [8]. There are many sources of uncertainties related to jet energy scale at CDF:

- Relative response of the calorimeters as a function of pseudorapidity.
- Single particle response linearity in the calorimeters.
- Fragmentation of jets.
- Modeling of the underlying event energy.
- Amount of energy deposited out of the jet cone.

The uncertainty on each source is evaluated separately as a function of the jet p_T (and η for the first uncertainty in the list above). Their contributions are shown in Fig. 1 for the region $0.2 < \eta < 0.6$. The black lines show the sum in quadrature (σ_c) of all contributions. This $\pm 1\sigma_c$ total uncertainty is taken as a unit of jet energy scale miscalibration (Δ_{JES}) in this analysis.

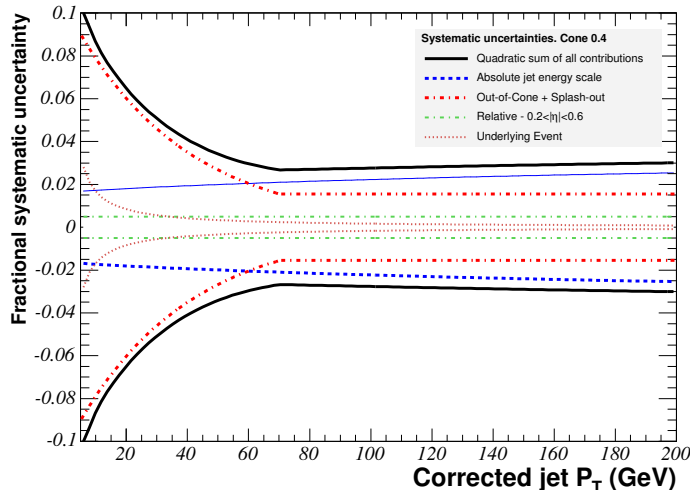


FIG. 1: Jet energy scale uncertainty as a function of the corrected jet p_T for the underlying event (dotted red), relative response (dashed green), out-of-cone energy (dashed red) and absolute response (dashed blue). The contribution of all sources are added in quadrature (full black) to form the total Δ_{JES} systematic σ_c .

V. EVENT RECONSTRUCTION

The event signature after event selection has a large missing transverse energy and big jet-multiplicities, and based on study from Monte Carlo samples we find that most of the selected events come from the $t\bar{t}$ lepton + jets decay channel, in which one of the W bosons from the top quark decay decays into two jets and the other into a lepton and a neutrino. We reconstruct the W boson mass from its hadronically decay jets to constrain *in situ* the jet energy scale (JES). For each possible jet-to-quark assignment of an event we calculate the invariant mass of two non-btagged jets, then we choose the one that has the value closest to the world average W mass measurement, 80.40 GeV/ c^2 , to be the reconstructed W mass called W_{jj} .

We reconstruct the top quark mass using a chi2 fitter that is similar to the old used in our 2.0 fb $^{-1}$ top mass analysis [4]. The modified chi2 fitter is defined as in Eqn. V.1, where we choose any combination of 4 jets out of all the jets in an event and use the missing E_T information to reconstruct m_t^{reco} :

$$\begin{aligned} \chi^2 = & \sum_{i=4\text{jets}} \frac{(p_T^{i,\text{fit}} - p_T^{i,\text{meas}})^2}{\sigma_i^2} + \sum_{j=x,y} \frac{(p_j^{UE,\text{fit}} - p_T^{UE,\text{meas}})^2}{\sigma_j^2} \\ & + \frac{(M_{jj} - M_W)^2}{\Gamma_W^2} \\ & + \frac{(M_{b,\text{missing}} - m_t^{\text{reco}})^2}{\Gamma_t^2} + \frac{(M_{bjj} - m_t^{\text{reco}})^2}{\Gamma_t^2} \end{aligned} \quad (\text{V.1})$$

where the first term constrains the p_t of the four jets to their measured values within their assigned uncertainties; the second term does the same for transverse components of unclustered energy; the third term constrains the invariant mass of two non-btag jets from W boson to be pole mass of W 80.42 GeV/ c^2 ; in the last two terms m_t^{reco} is the free parameter for the reconstructed top quark mass used in the minimization, M_{bjj} is the invariant top mass from a candidate b -jets and two non-btag jets, and $M_{b,\text{missing}}$ is the invariant mass from another candidate b -jet and the missing momentum information. Here the missing momentum information does not only contain the neutrino but also the undetected lepton information.

As mentioned in the Event Selection section, the signal region of this analysis requires the number of jets to be between 4 and 6. Since we choose only 4 jets to reconstruct the top quark mass, we treat the events with exactly 4 jets differently from those events with 5 or 6 jets during event reconstruction. For instance, if an event has 5 jets, we have 5 different ways to choose 4 jets out of 5, and the final reconstructed top quark mass from the chi2 fitting is the one that has the minimum of all possible jet choices.

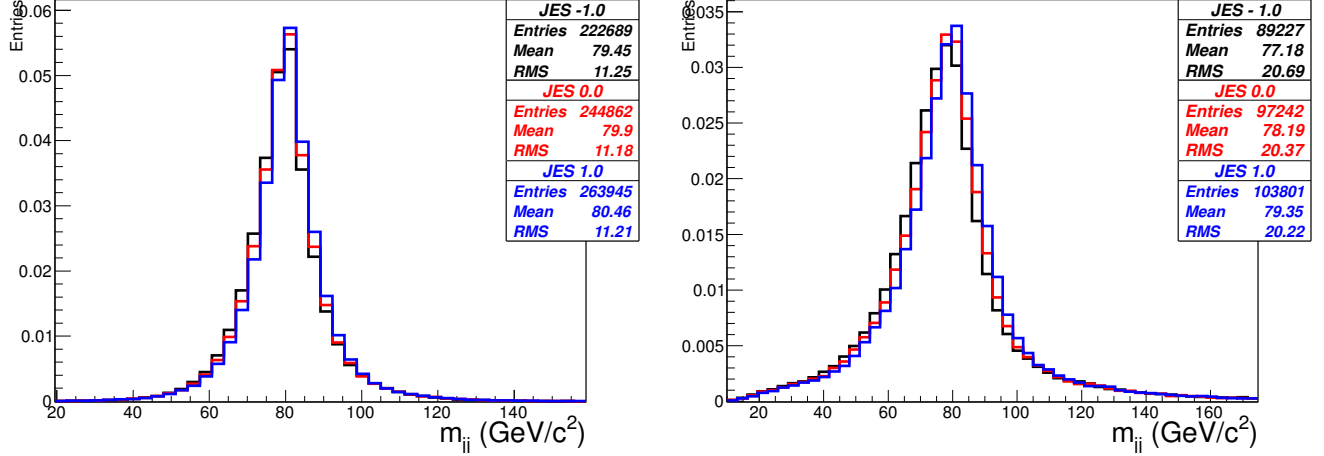


FIG. 2: Distribution of reconstructed m_{jj} with different input JES's, after all cuts are applied, both 1tag (left) and 2tag (right) are shown.

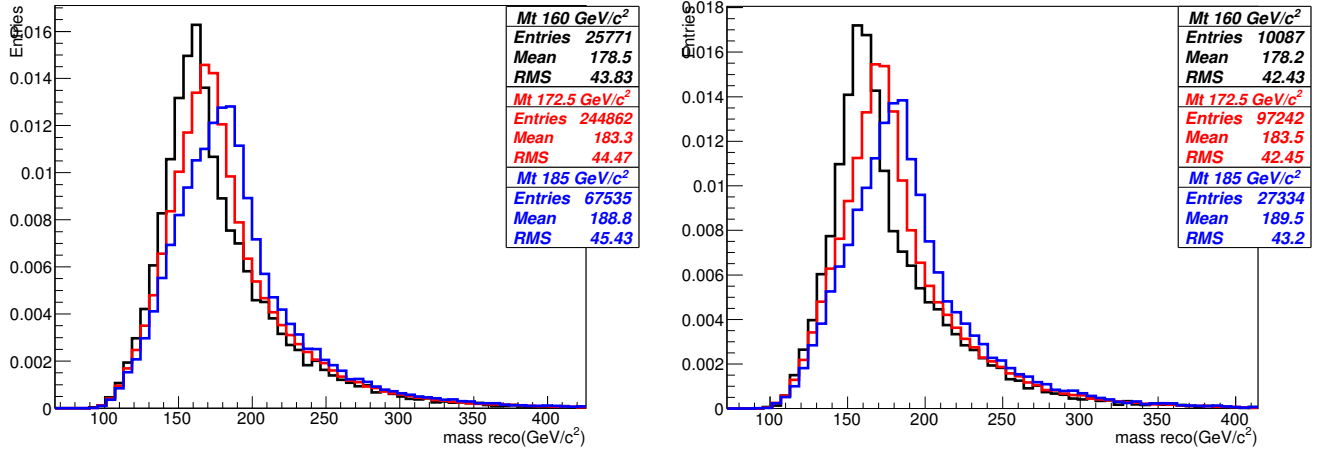


FIG. 3: Distribution of reconstructed m_t^{reco} with different input top quark masses, after all cuts are applied, both 1tag (left) and 2tag (right) are shown.

We minimize the chi2 fitter above and choose the fitted mass corresponding to the minimal chi2 as our reconstructed top quark mass. In order to extract more information from each event, we further reconstruct a 2nd top mass $M_t^{\text{reco}(2)}$, which is chosen from the second-best chi2 fitted mass during the reconstruction of m_t^{reco} . To give a sense of how the resolution power of these observables behaves, Figure 2 shows the distribution of m_{jj} with different input ΔJES values, while the input top mass is the same for all of them ($M_t = 172.5 \text{ GeV}/c^2$). Figure 3 and Figure 4 show the distribution of reconstructed m_t^{reco} and $M_t^{\text{reco}(2)}$, with different input top quark masses, while the input ΔJES is the same. These different distributions are named *templates* of the analysis, which are the basis of the method of our top mass measurement.

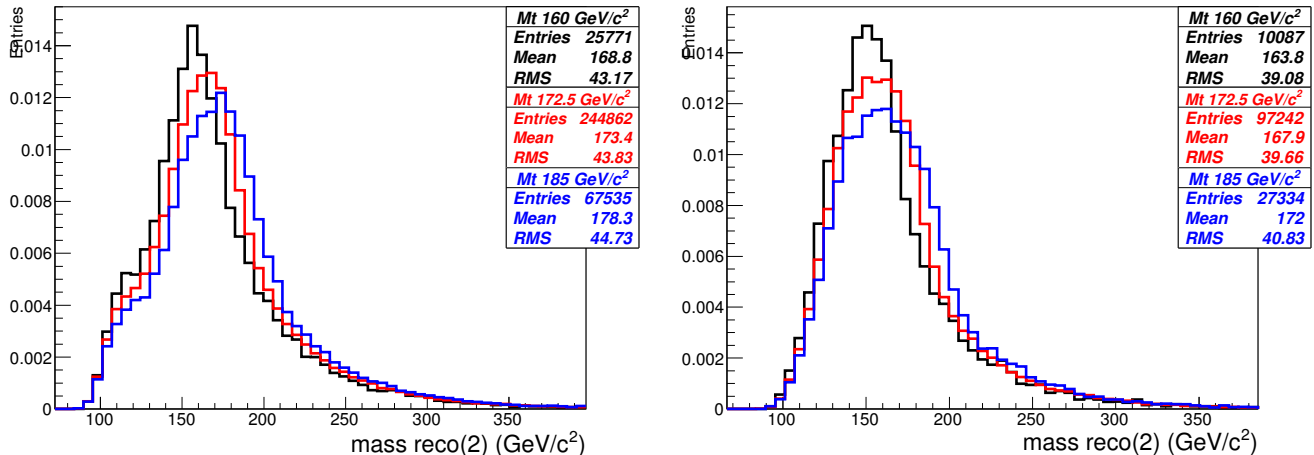


FIG. 4: Distribution of reconstructed $M_t^{\text{reco}(2)}$ with different input top quark masses, after all cuts are applied, both 1tag (left) and 2tag (right) are shown.

VI. KERNEL DENSITY ESTIMATES

Probability density functions for $m_t^{\text{reco}}, M_t^{\text{reco}(2)}$, and m_{jj} at every point in the signal $M_{\text{top}} - \Delta_{\text{JES}}$ grid and for backgrounds are derived using a Kernel Density Estimate (KDE) approach. KDE is a non-parametric method for forming density estimates that can easily be generalized to more than one dimension, making it useful for this analysis, which has three observables per event. The probability for an event with observable (x) is given by the linear sum of contributions from all entries in the MC:

$$\hat{f}(x) = \frac{1}{nh} \sum_{i=1}^n K\left(\frac{x-x_i}{h}\right). \quad (\text{VI.1})$$

In the above equation, $\hat{f}(x)$ is the probability to observe x given some MC sample with known mass and JES (or the background). The MC has n entries, with observables x_i . The kernel function K is a normalized function that adds less probability to a measurement at x as its distance from x_i increases. The smoothing parameter h (sometimes called the bandwidth) is a number that determines the width of the kernel. Larger values of h smooth out the contribution to the density estimate and give more weight at x farther from x_i . Smaller values of h provide less bias to the density estimate, but are more sensitive to statistical fluctuations. We use the Epanechnikov kernel, defined as:

$$K(t) = \frac{3}{4}(1-t^2) \text{ for } |t| < 1 \text{ and } K(t) = 0 \text{ otherwise,} \quad (\text{VI.2})$$

so that only events with $|x-x_i| < h$ contribute to $\hat{f}(x)$. We use an adaptive KDE method in which the value of h is replaced by h_i in that the amount of smoothing around x_i depends on the value of $\hat{f}(x_i)$. In the peak of the distributions, where statistics are high, we use small values of h_i to capture as much shape information as possible. In the tails of the distribution, where there are few events and the density estimates are sensitive to statistical fluctuations, a larger value of h_i is used. The overall scale of h is set by the number of entries in the MC sample (larger smoothing is used when fewer events are available), and by the RMS of the distribution (larger smoothing is used for wider distributions). We extend KDE to two dimensions by multiplying the two kernels together:

$$\hat{f}(x,y) = \frac{1}{n} \sum_{i=1}^n \frac{1}{h_{x,i}h_{y,i}} \left[K\left(\frac{x-x_i}{h_{x,i}}\right) \times K\left(\frac{y-y_i}{h_{y,i}}\right) \right]. \quad (\text{VI.3})$$

Figures 5 shows the 2d density estimates of signal events for each pair of the three observables, for events with exactly 4 jets only. Fig. 6 shows the same type of density estimation for events with 5 or 6 jets.

VII. LIKELIHOOD FIT

The template method uses a multi-dimensional likelihood function fitting to find the most probable top mass given the data samples. We divide the original data samples into subsamples of 1btag and 2btag events separately, and for each subsample we define a likelihood function with the following format:

$$\mathcal{L}_{\text{shape}} = \frac{\exp(-(n_s + n_b))(n_s + n_b)^N}{N!} \times e^{-\frac{(n_{b0} - n_b)^2}{2\sigma_{n_{b0}}^2}}$$

$$\times \prod_{i=1}^N \frac{n_s P_s(m_t^{\text{reco}}, M_t^{\text{reco}(2)}, m_{jj}; M_{\text{top}}, \Delta_{\text{JES}}) + n_b P_b(m_t^{\text{reco}}, M_t^{\text{reco}(2)}, m_{jj})}{n_s + n_b}$$

where n_s and n_b are signal and background expectations and N is the number of events in the sample, P_s is the signal probability density function and P_b is the background probability density function. The first term in the likelihood is present because this is an extended maximum likelihood, in which the numbers of signal and background events obey Poisson statistics. The second term in the product expresses the Gaussian constraints on the background expectation. We use the *a-priori* estimate n_{b0} and its uncertainty $\sigma_{n_{b0}}$ to improve sensitivity. Shape information is used in the third term where probability density functions are used to discern between signal and background events and to extract mass information. A term like this exists for each of the two subsamples, and the final likelihood function is a product of them. We also impose a unit Gaussian constraint on Δ_{JES} .

The above gives the likelihood value only for points in the $M_{\text{top}} - \Delta_{\text{JES}}$ grid, and not as a continuous function. To obtain density estimates for an arbitrary point in the $M_{\text{top}} - \Delta_{\text{JES}}$ grid, we use local polynomial smoothing on a per-event basis. The value of the density estimate is obtained for an event at the available points, and a quadratic fit is performed in $M_{\text{top}} - \Delta_{\text{JES}}$ space, where the values of M_{top} and Δ_{JES} far away from the point being estimated are deweighted. This allows for a smooth likelihood that can be minimized. The measured uncertainty on M_{top} comes from the largest possible shift in M_{top} on the $\Delta \ln \mathcal{L} = 0.5$ contour.

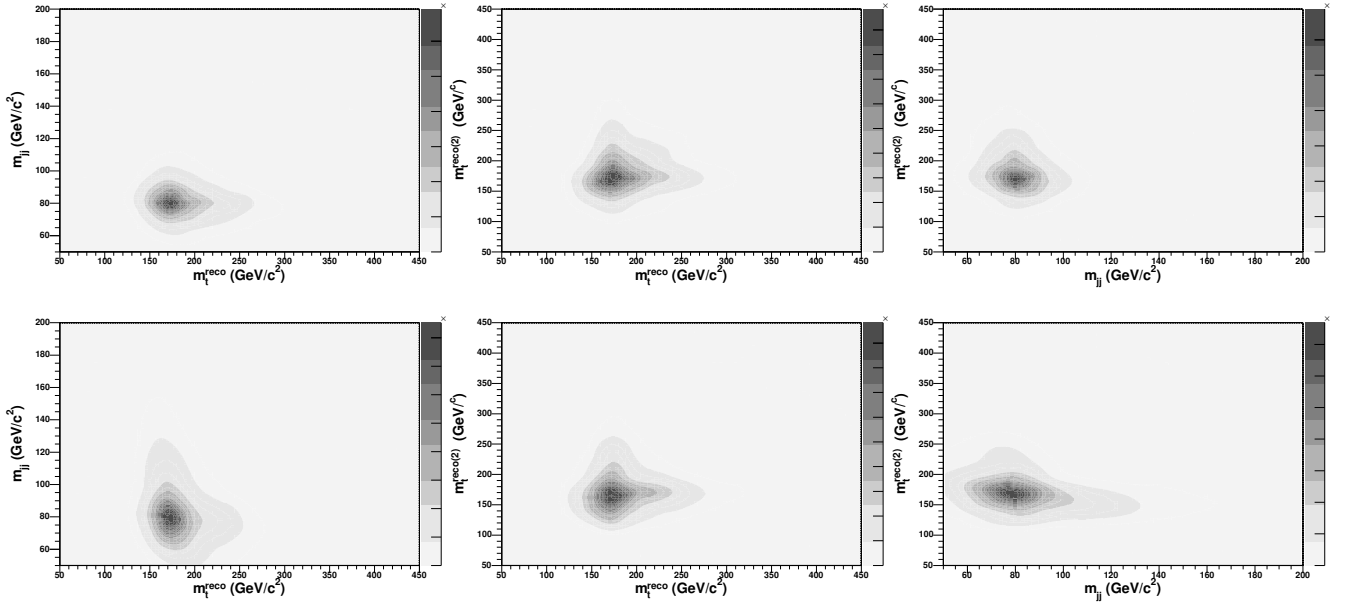


FIG. 5: Full 2d density estimates for input mass of $171.5 \text{ GeV}/c^2$ and $\Delta_{\text{JES}} = 0.0$ for 1-tag events (up) and 2-tag events (down).

VIII. METHOD CHECK

It is possible that our method has biases to the measured top quark mass. To estimate the bias, we run pseudo-experiments (PE) on signal samples with different input M_{top} and Δ_{JES} . Since the background sample is estimated from real data events, we use the same background events for different MC signal samples when running PE's. The number of background events used to run PE is the number we obtain from background estimation, while the number of signal events drawn to run PE is calculated from the theoretical calculation with cross section of $\sigma = 7.4$ pb, at $M_{top} = 172.5$ GeV/c^2 .

Figure 7 shows that our method biases the top mass to a certain degree. We use a linear function to fit the measured top mass vs the input top mass, and apply this linear fit as a calibration to our measured top quark mass. Figure 8 shows the biascheck and pull width plots after calibration, and the constant fitting lines on both plots tell us that after calibration the measured top mass well matches the input top mass and that we have a reasonable estimated statistical uncertainty on top mass measurement.

We then inspect the measured top mass dependencies on Δ_{JES} . Three top mass MC samples are chosen: $M_{top} = 167.5$ GeV/c^2 , 172.0 GeV/c^2 , and 177.5 GeV/c^2 , each with five different Δ_{JES} : $0.0, \pm 0.4, \pm 1.0$. By applying the same calibration described above, we get the plots shown on Fig. 9. The left plot of Fig. 9 shows a non-zero shift of measured top mass regarding the Δ_{JES} dependency, and to be conservative, we take half the difference of the maximum and minimum shift of measured top mass as a systematic contribution to this analysis, which is around 0.4 GeV/c^2 . Figure 10, which presents the biascheck of measured Δ_{JES} vs input Δ_{JES} , after calibration, also shows a good agreement between the measured Δ_{JES} and input Δ_{JES} after calibration.

IX. FIT RESULTS

With the likelihood function we now can fit the data. Figure 11 is the two-dimensional likelihood fit for data, from which we measure (after the calibration)

$$\begin{aligned} M_{top} &= 171.3 \pm 1.4 \text{ GeV}/c^2, \text{ calibrated} \\ \Delta_{JES} &= 0.2 \pm 0.2 \end{aligned}$$

Figure 12 and Fig. 13 show the three kinematic variables from data, overlaid with their corresponding one-dimensional p.d.f's from a MC sample with input $M_{top} = 171.5$ GeV/c^2 and $\Delta_{JES} = 0.0$, plus the background

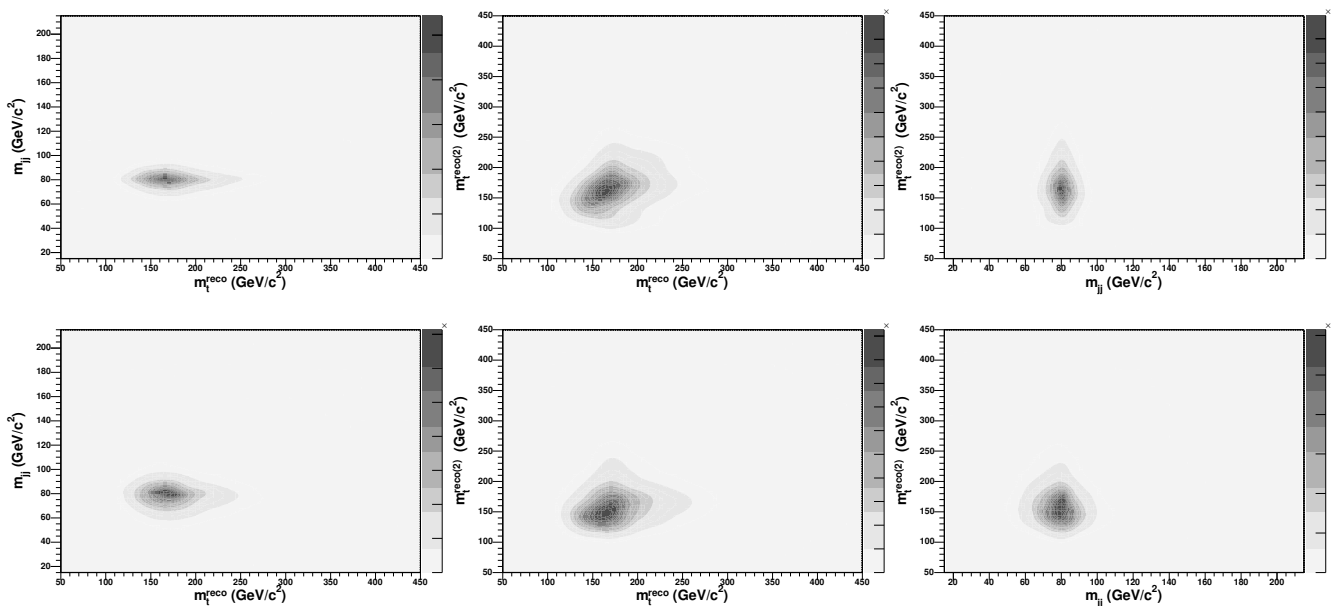


FIG. 6: Full 2d density estimates for input mass of 171.5 GeV/c^2 and $\Delta_{JES} = 0.0$ for 1-tag events (up) and 2-tag events (down).

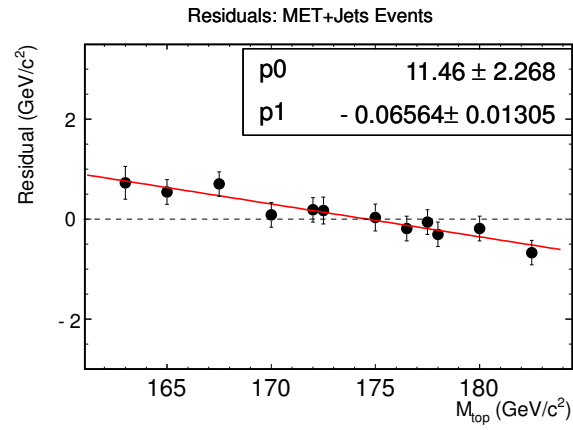


FIG. 7: Biaschecks of the measured top quark mass before any correction/calibration. All the MC samples have the same $\Delta_{\text{JES}} = 0.0$.

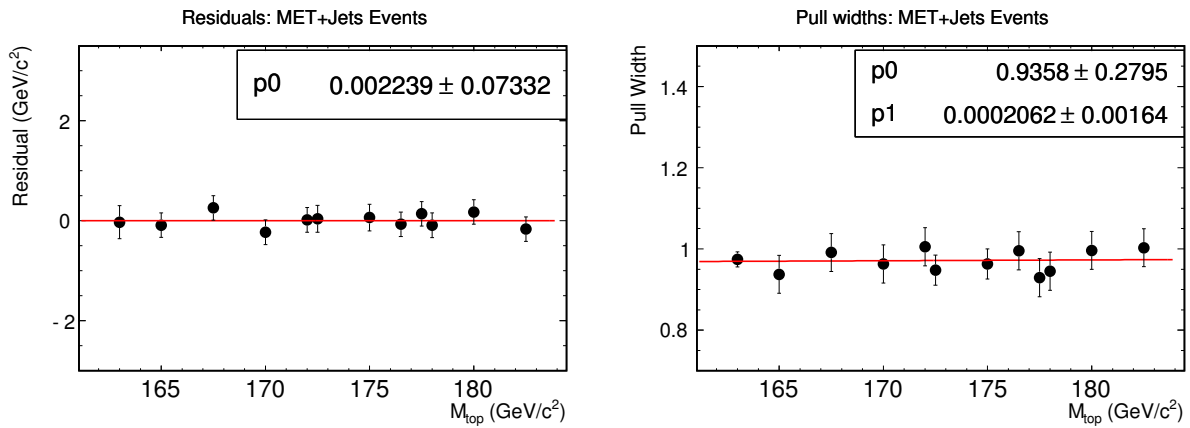


FIG. 8: Biaschecks of the measured top quark mass after calibrations. Residual plot is on the left, and the pullwidth plot on the right. All the samples have the same $\Delta_{\text{JES}} = 0.0$.

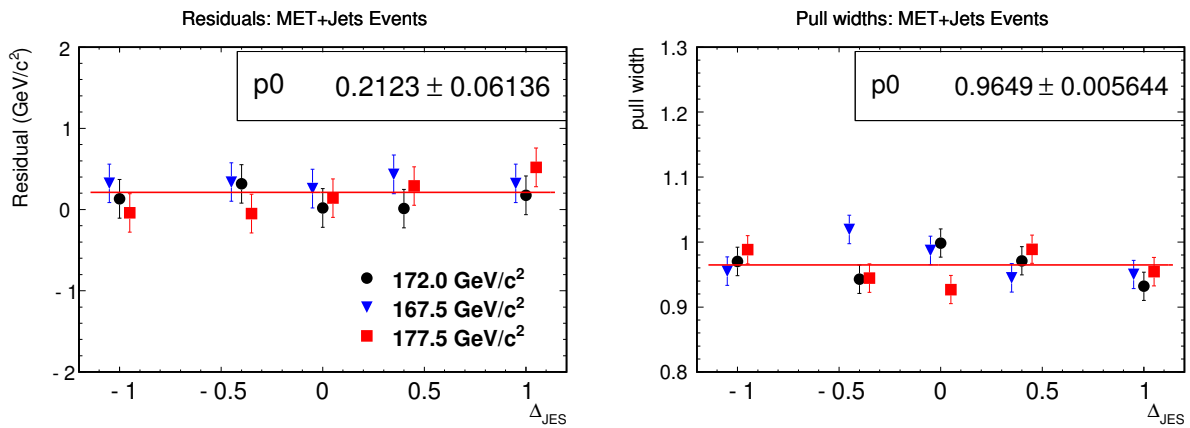


FIG. 9: Checks of the measured top mass dependencies on the Δ_{JES} . Plots shown here are after calibration.

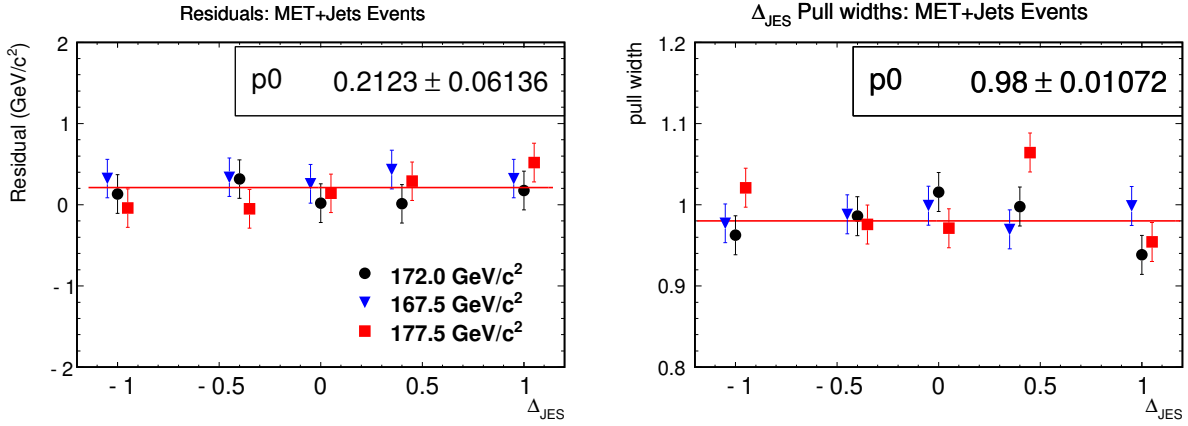


FIG. 10: Biaschecks of the measured Δ_{JES} vs the input Δ_{JES} . Different color represents different input top masses.

fully modeled.

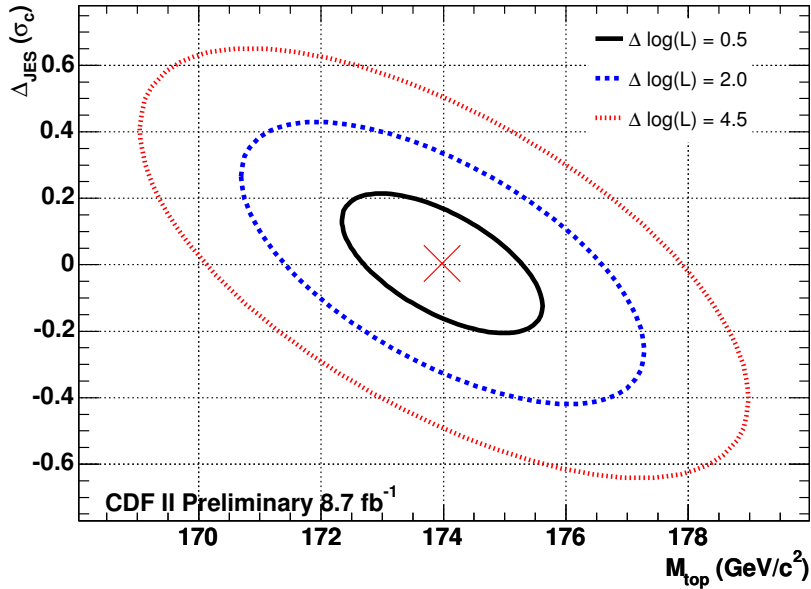


FIG. 11: 2D likelihood fit contours for the data fitting.

X. SYSTEMATIC UNCERTAINTIES

We examine a variety of effects that could systematically shift our measurement. As a single nuisance parameter, the JES that we measure does not fully capture the complexities of possible jet energy scale uncertainties, particularly those with different η and p_T dependence. Fitting for the global JES removes most of these effects, but not all of them. We apply variations within uncertainties to different JES calibrations for the separate known effects in both signal and background pseudodata and measure resulting shifts in M_{top} from pseudoexperiments, giving a residual JES uncertainty. We also vary the energy of b jets, which have different fragmentation than light quarks jets, as well as semi-leptonic decays and different color flow, resulting in a b-JES systematic. Effects due to uncertain modeling of radiation including initial-state radiation (ISR) and final-state radiation (FSR) are studied by extrapolating uncertainties in

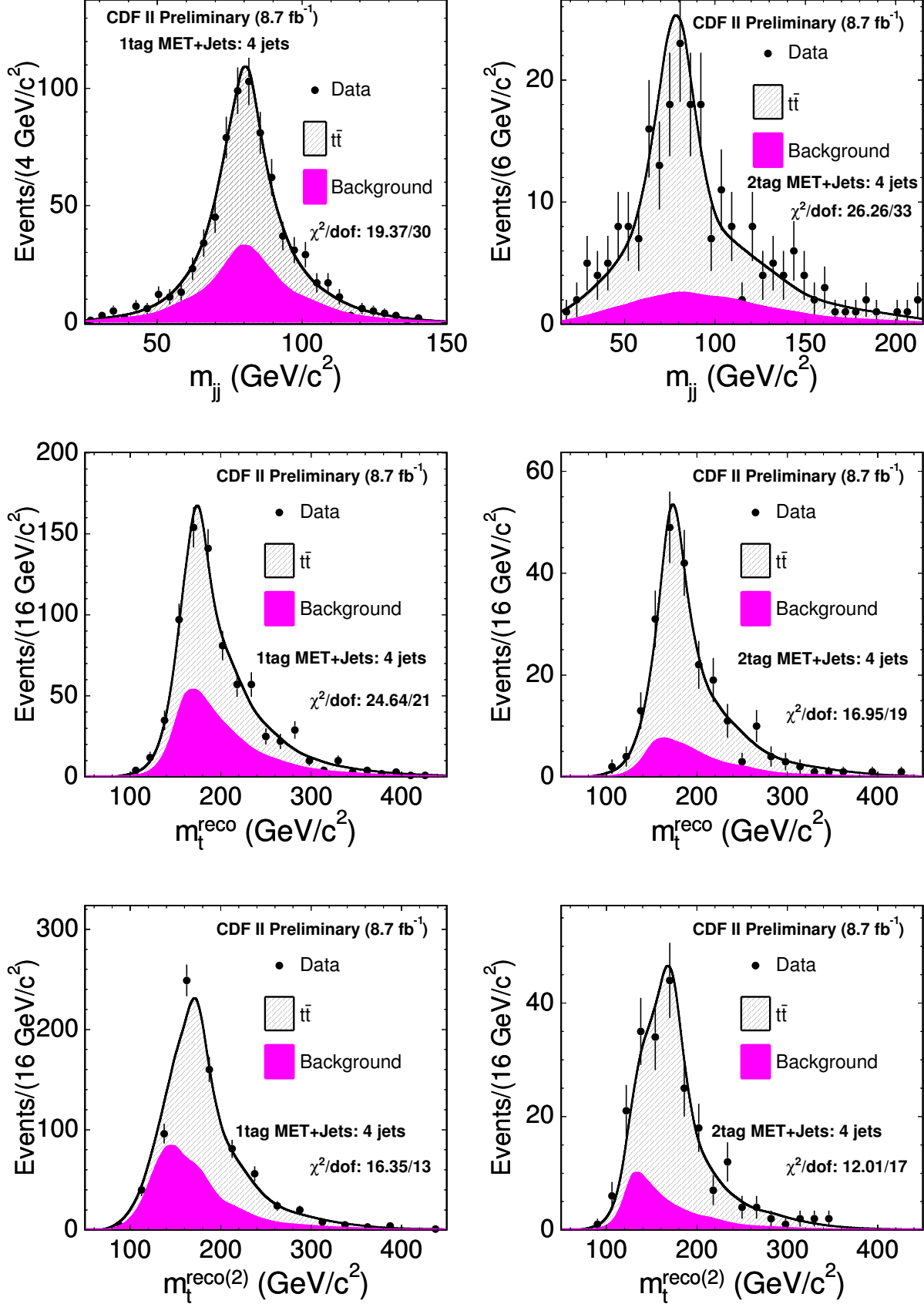


FIG. 12: Distribution of kinematic variables m_t^{reco} , W_{jj} , and $M_t^{\text{reco}(2)}$ from data, overlaid with their corresponding 1-d p.d.f.'s from MC sample $ykt71$ (with input $M_{top} = 171.5 \text{ GeV}/c^2$ and $\Delta_{JES} = 0.0$) plus the background fully modeled. Each event here contains exactly 4 jets, both 1tag (left) and 2tag (right) events are displayed.

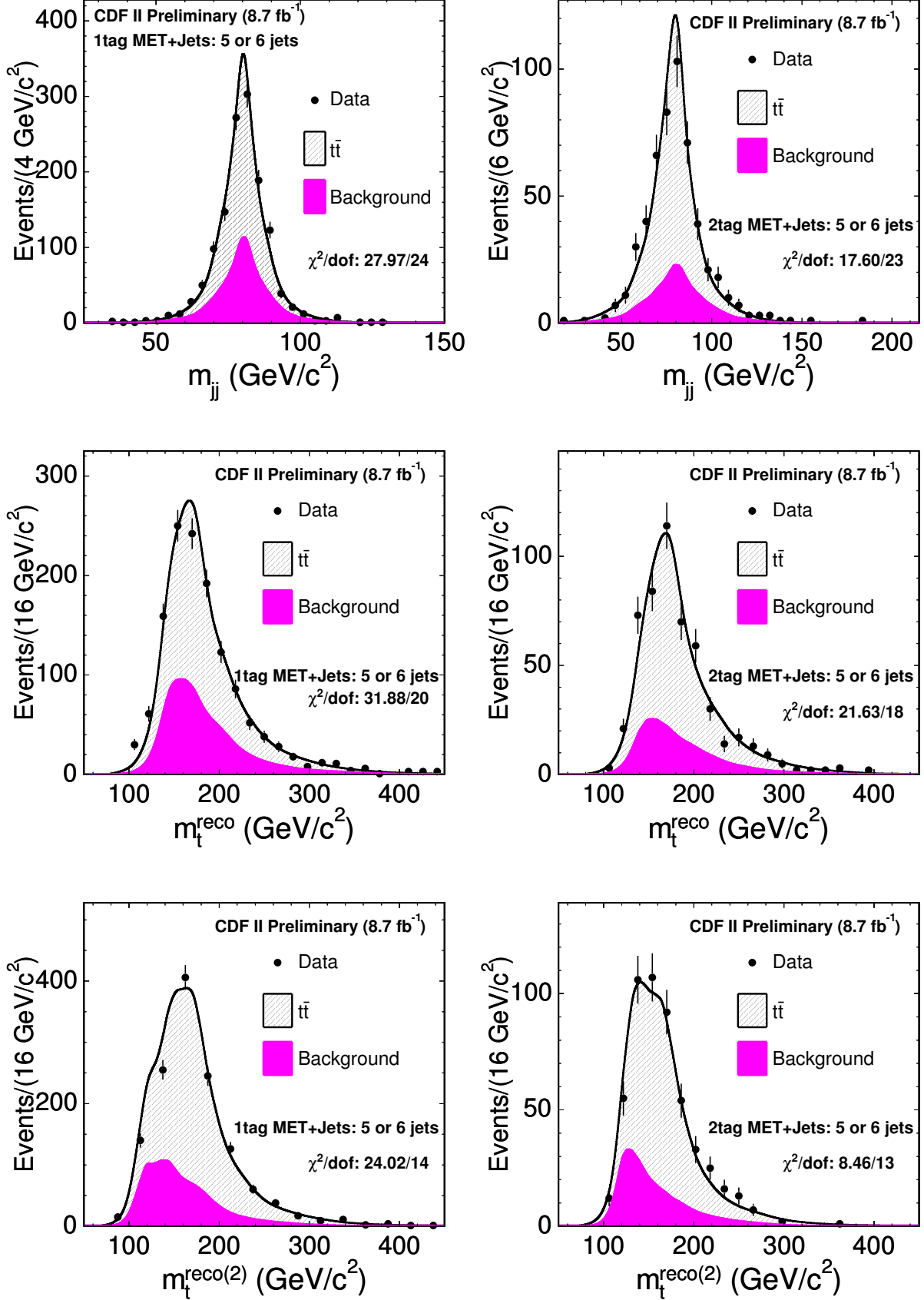


FIG. 13: Distribution of kinematic variables m_t^{reco} , W_{jj} , and $M_t^{\text{reco}(2)}$ from data, overlaid with their corresponding 1-d p.d.f.'s from MC sample $ykt71$ (with input $M_{top} = 171.5 \text{ GeV}/c^2$ and $\Delta_{JES} = 0.0$) plus the background fully modeled. Each event here contains 5 or 6 jets, both 1tag (left) and 2tag (right) events are displayed.

TABLE III: Summary of systematic effects. All numbers are after calibration.
CDF II Preliminary 8.7 fb^{-1}

Systematic	$\Delta M_{top} \text{ (GeV}/c^2)$
Residual JES	0.4
Generator	0.4
PDFs	0.2
b jet energy	0.2
Background	0.2
gg fraction	0.3
Radiation	0.3
Trigger simulation	0.1
Multiple Hadron Interaction	0.2
Color Reconnection	0.3
Calibration	0.2
Total Effect	0.9

the p_T of Drell-Yan events to the $t\bar{t}$ mass region, resulting in a radiation systematics. Comparing pseudoexperiments generated with HERWIG and PYTHIA gives an estimate of the generator systematic. A systematic on different parton distribution functions is obtained by varying the independent eigenvector of the CTEQ6M set, comparing parton distribution functions with different values of Λ_{QCD} , and comparing CTEQ5L with MRST72. We also test the effect of reweighting MC to increase the fraction of $t\bar{t}$ events initiated by gg (vs qq) from the 6% in the leading order MC to 20%. Systematic effects due to the background modeling and trigger simulation are also taken into account. The color reconnection effects are accounted by generating new MC sample which have color effects. As mentioned in the bias check section, since the bias of measured top mass has non-zero shift regarding the JES dependency, we also take this effect into account when evaluating systematic effects.

The total systematic error is $0.9 \text{ GeV}/c^2$, summarized in Table III.

XI. CONCLUSIONS

We present a measurement of the top quark mass using events that have a signature of MET + high jet-multiplicities with a template-based technique. An *in situ* JES calibration is used to constrain the jet energy scale. Using three dimensional templates derived from Kernel Density Estimation and 8.7 fb^{-1} of full CDF data, we measure

$$\begin{aligned}
 M_{top} &= 173.9 \pm 1.6 \text{ (stat. + JES)} \pm 0.9 \text{ (syst.) GeV}/c^2 \\
 &= 173.9 \pm 1.9 \text{ GeV}/c^2 \\
 \Delta_{JES} &= 0.0 \pm 0.2\sigma_c
 \end{aligned}$$

Acknowledgments

We thank the Fermilab staff and the technical staffs of the participating institutions for their vital contributions. This work was supported by the U.S. Department of Energy and National Science Foundation; the Italian Istituto Nazionale di Fisica Nucleare; the Ministry of Education, Culture, Sports, Science and Technology of Japan; the Natural Sciences and Engineering Research Council of Canada; the National Science Council of the Republic of China; the Swiss National Science Foundation; the A.P. Sloan Foundation; the Bundesministerium fuer Bildung und Forschung, Germany; the Korean Science and Engineering Foundation and the Korean Research Foundation; the Particle Physics and Astronomy Research Council and the Royal Society, UK; the Russian Foundation for Basic Research; the Comision Interministerial de Ciencia y Tecnologia, Spain; and in part by the European Community's

Human Potential Programme under contract HPRN-CT-20002, Probe for New Physics.

- [1] F. Abe, et al., Nucl. Instrum. Methods Phys. Res. A **271**, 387 (1988);
- [2] T. Aaltonen et al., Phys. Rev. Lett. 107, 232002 (2011);
- [3] A. Abulenci et al., Phys. Rev. D 73, 032003 (2006);
- [4] T. Aaltonen et al., Phys. Rev. D 79, 092005(2009);
- [5] A. Abulenci et al., Phys. Rev. Lett. 96, 022004 (2006);
- [6] F. Abe, et al., Phys. Rev. D 45, 1448 (1992);
- [7] T. Affolder, et al., Phys. Rev. D 64, 032002 (2001);
- [8] A. Bhatti, et al., Nucl. Instrum. Methods Phys. Res. A **566**, 375 (2006);